Phased array measurements under dynamic conditions

Jon Martens

[Summary] Among phased array measurements of interest are studies of what happens to the radiation pattern as the array transitions from one beam angle to another. The time scales and magnitudes of effects can vary significantly depending on the array details: radiation may instantaneously appear in unexpected directions, distortion products may change and the beam shape may be altered. A network/signal analysis measurement approach based on sufficiently fast acquisition, multiple receivers, and flexible triggering schemes can allow for this kind of transient information to be captured with relatively controlled uncertainties.

1 Introduction

For 5G/6G and related applications and, for other situations with increasing radio integration, measurements of phased array systems and subsystems have become increasingly important[e.g., 1)-2)]. Considerable work has been done looking at over-the-air (OTA) measurements[e.g., 3)-5)] in areas such as

- beam steering,
- pattern measurements,
- analysis of loss, efficiency and bandwidth,
- error-vector magnitude and bit/frame error rates

Some of these studies have focused on transient effects during beam steering[5)] where the timing details of how the beam settles to its new position may be critical to overall system latencies and other performance factors. The time scales of interest may vary widely depending on the system. Some may settle on the order of seconds or longer while others may require resolution on the nanosecond scale. While the former measurements may relatively straightforward to orchestrate on many instruments, the faster measurements may require sampling schemes, such as discussed elsewhere[5)], or measurement receivers with wide IF bandwidths and high-rate digitizers (to be focused on here). All will require triggering capabilities to allow timing alignment with beam motion and, of course, these become more complicated as the rates of motion increase.

In addition to the above studies, the dynamics of distortion products may also be of interest as the products may radiate in different directions[6)] than the main beam (even statically but potentially more so during transitions[7)]) and the time settling during transitions may be very different from that of the linear signal components. Such deviations may have regulatory or overall system performance implications further suggesting the value of a more complete measurement approach.

This paper will explore a collection of measurement processes to look at the behaviors of both linear and less-than-linear signal components during a phased array beam transition in a configuration loosely described by Figure 1. The measurement hardware, covering a variety of receiver, acquisition and triggering configurations, will be presented along with an analysis of the uncertainty picture. The measurement class will be studied through a series of examples at both FR2 frequencies and higher in the mm-wave range to look at some physical mechanisms of potential interest and the measurement capabilities that might be possible.

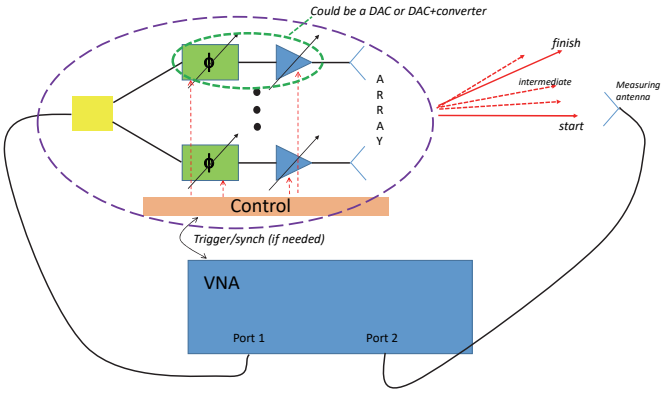

Figure 1 A simplified diagram of dynamic array measurements using a VNA. The phased array is shown as having discrete phase shifters and amplitude controls but other levels of integration are possible. Different receivers and different signal types could be employed as could a moving or phased array measuring antenna.

2 Instrumentation and DUT structure

Many different measurement platforms could be used to capture the dynamic events discussed above. Some requirements include a sufficiently fast acquisition rate to capture the quantities of interest (but this can be mitigated by fast sweeping receiver arrays or multiple receivers), adaptable triggering to respond to state changes in the DUT or other measurement parameters, sufficient dynamic range to deal with path losses that may be encountered and possibly multiple receivers to deal with multiple polarizations or site locations. Such an instrument can be described in network analysis or signal analysis terms but this paper will focus on the former. A block diagram of such a configuration is in Figure 2 and is based on a MS4640 VNA platform where a fast digitizing option with deep memory is available and mm-wave extension heads can be used for measurements above 70 GHz (either from Anritsu[8] or from other vendors). The mm-wave modules share the base source and LO synthesis paths and their IF signals multiplex onto the same IF paths of the instrument so the performance attributes are similar (aside from differences in available port power and front-end noise floor).

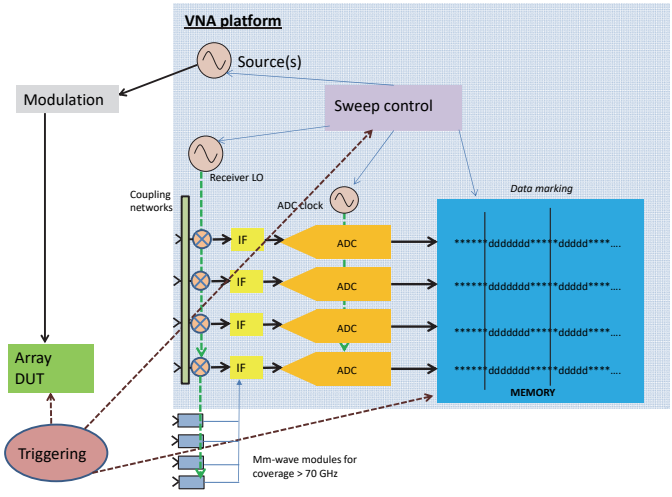

Figure 2 A simplified block diagram of a VNA structure used for the array measurements. Different IF subsystems, different RF front ends and different triggering options are sometimes needed.

The fast digitizing IF permits acquisition times as fast as 2.5 ns and with 8+ GB of memory, relative long time records can be retained to allow analysis of transient events (up to 2 seconds at the highest sampling rate, minutes at slower rates)[9]. In the VNA's native form (without the fast digitizing option), acquisition times are limited to a few μs but can be processed real-time. A variety of triggering schemes are also sketched in the figure. If sufficiently slow (of order ms), the acquisition hardware can be triggered directly. If much faster, the events can be marked in the deep memory of the digitizer with a timing resolution of as small as 5 ns.

The measurement uncertainties in any over-the-air measurement can present a complex picture and the class of analysis presented here is no different. Among the components:

- Noise floor (which is affected strongly by path losses). This may be relevant in larger setups and/or wider beamwidths with low power transmitters. Pre-amplification and coupler bypass (in the case of VNAs) can provide some benefit. IF bandwidths/RBW reduction can be used to improve the results but degrade acquisition speed. Without pre-amplifiers or coupler bypass, noise floors may be in the −110 to −130 dBm range at FR2 frequencies (in relative wide IF bandwidths) and −100 to −120 above 70 GHz for conventional acquisition systems. For the fast digitizing option being discussed, the floors may be 10-20 dB higher.
- Receiver linearity and power accuracy. For relative measurements (most pattern measurements and IMD in dBc terms, for example), receiver linearity is the more important quantity but these impacts are generally <0.05 dB for typical OTA level ranges (unless receive-plane power is very high). For absolute level measurements, power sensor accuracy must be transferred to the receiver where repeatability (see below) and match correction (between source, receiver and sensor) comes into play.
- Mechanical repeatability. This often can be a dominant term at FR2 and higher frequencies as the mechanical precision required on mounting and positioning can be severe. For the present experiments, this was the largest component of uncertainty (even for a static setup).

The net result was two-sigma uncertainties (in the FR2 frequency ranges) on the order of 0.7 dB at the −80 dBm absolute level (about the lowest IMD product measurements seen in this work, other signal levels were higher except in the E/W-band case) decreasing to 0.4 dB at the −30 dBm level.

Several different DUTs will be used in the example measurements. One is a 4×4 microstrip patch array designed for FR2 operation centered at 28 GHz. Each element has independent gain and phase control (with 0.5 dB and 1 degree

control precision) and separate power amplifiers. Another DUT is a linear array designed for operation at E/W-band with synthesized phase and amplitude control (coming from microwave baseband, with 0.01 dB and 0.1 degree control precision, and upconverted).

3 Measurement results and examples

Starting with the 4×4 array, a zoomed-in view of the pattern transition for a 1 degree main beam movement is shown in Figure 3 at 28 GHz. Since the time scale was relatively slow for this array, a traditional receiver structure was used with hardware synchronization of the beam motion activation. The path losses were on the order of 40 dB in this case so dynamic range limitations were not really an issue (and IFBW of 10 kHz could easily be used). As the path losses increase, hardware additions (pre-amplifiers) or acquisition changes (faster IF paths) may be needed.

The first element changes state (after some control latency) at about the 30.6 ms time mark and the last element has settled into its new state at about the 35.4 ms time mark. In between, one can see that there are a variety of changes in level detected at the fixed observation angle with deviations approaching 1 dB in places. The details of the energy variation at one-point and the beam maximum levels at other angles may determine if this is an issue or not for a given system.

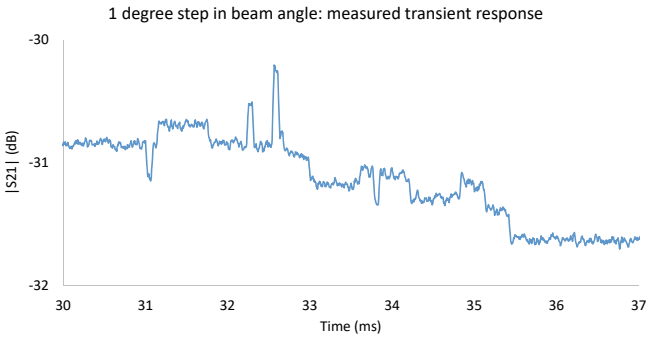

Figure 3 The measured response at the probe antenna is shown as the phased array beam makes a 1 degree transition. The array is a 4×4 structure operating near 28 GHz.

Since the main beam structure can vary during these transition periods, a different way of looking at the data may be helpful. A trajectory diagram is one possibility and one is shown in Figure 4. Here, the location of the main beam peak (defined as the maximum), the maximum level of that peak and the beamwidth are collected at (relatively) closely spaced points in time during the transition and plotted in 3D space. The starting and ending points (with a 1 degree beam shift and roughly equal amplitudes and beamwidths) are shown but the path traversed in this case covers quite a bit of territory. Depending on the array structure and programming behaviors, very different trajectories might be observed.

Relative to Figure 3, more spatial points had to be acquired per time step which raised some acquisition complications. In this case, multiple receivers sampling simultaneously were used (the positions were tailored for the particular measurement). Alternatively, a faster phased array could have been used to sweep the region of interest. The absolute path losses were still not extreme in this case (to 50 dB) so noise floor limits were not dominant although trace noise levels did increase.

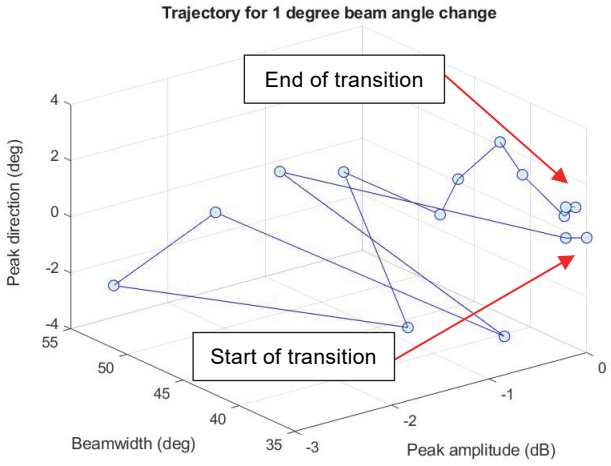

Figure 4 The trajectory of an example array's 1 degree beam position transition is shown in more detail.

An E/W-band linear phased array was also examined using this class of methods. This array's transition speed was higher than in the previous examples so the faster digitizing IF scheme was employed for the measurement. A 10 degree change in beam angle was excited and the received response at a fixed point is shown in Figure 5. The elements in this array were direct DAC-like structures (and upconverted) unlike the discrete phase shifters in the previous example. The trajectory is more complicated due to the nature of the programming but, once the last event had been sent, the pattern settled within about 15 μs. Far faster arrays exist but the measurement hardware described here could be used for transition times into the 10 s of nanoseconds. The uncertainty on the data is higher on this example for noise floor

reasons as transmit power was relatively low and the path losses were quite high at 77 GHz (approximately 1.5 dB net uncertainty).

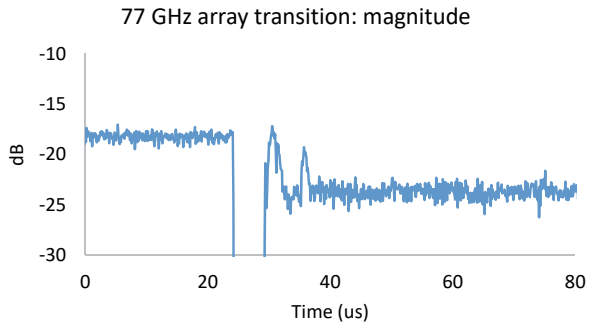

Figure 5 The response of an E/W-band array 10 degree beam angle transition is shown here on a faster time scale.

To help with discussion of less-than-linear dynamics, it may be useful to first look at the beam creation itself. Depending on the architecture of a given phased array system, a calibration (in terms of the phase shifter and amplitude control settings, by element, for a given beam direction) can be frequency dependent. An example of this is shown in array beam patterns in Figure 6 where a single set of calibration values was used for a number of different carrier frequencies[7]. Small steps appear in the data because of finite programming resolution for the array (1 degree increments). Because of the observed frequency dependence, for modulation of more than to 100 MHz bandwidth, some beam distortion can be expected without compensation efforts. Since distortion products will be even further from the carrier, generally, larger beam divergences for those components might be expected. Even without dynamic effects, this latter behavior can be interesting from an interference perspective.

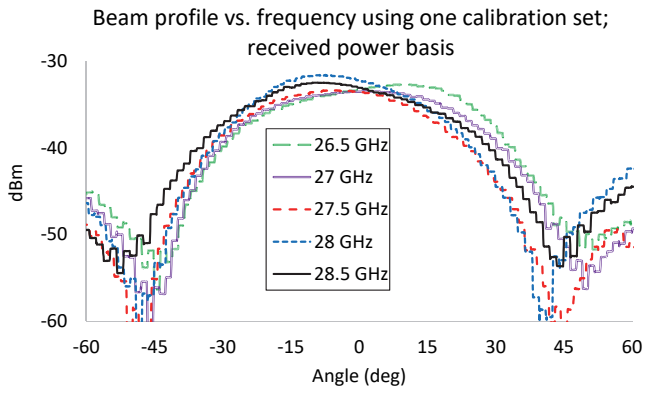

Figure 6 The patterns of a 4×4 phased array at four different frequencies are shown where a single set of array calibration coefficients were used[7]. The differences in curves suggest the frequency dependence of the calibration.

As an example of these beam divergence/distortion effects, patterns are shown both for a main tone and for some third order distortion products, with a tone spacing of 100 MHz, in Figure 7 for an example 4×4 FR2 array. The peak levels are normalized and the scales offset for clarity. When the average amplifier in the array is compressed by 1 dB, note that the main tone beam does not change peak direction substantially but the lobe width is altered as the element amplifiers compress by different amounts. The peak direction for the 3rd order distortion product is not aligned with the main tone even when backed-off. This may not be surprising based on the calibration frequency dependence. When 1 dB compressed, the distortion peak direction actually changes to the other side of the main tone and the lobe changes shape. It is believed that this is principally due to the different elements compressing at slightly different rates. Inter-element coupling and associated 'load pull' can also play a role in certain phased array systems[6), 10)].

A dynamic look at the intermodulation product during beam sweep may also be interesting (Figure 8). The beam was swept in 1 degree steps. The pattern is not particularly symmetric as levels of distortion in the elements are not consistent and there may be some angular dependence. In addition, one can detect transient overshoot in places (between the 200 and 400 ms time stamps) which appear to again be related to different elemental settling times and a resulting change in summation of individual distortion products. Observationally, this behavior is highly dependent on the element design details and the presence of any nonlinear coupling.

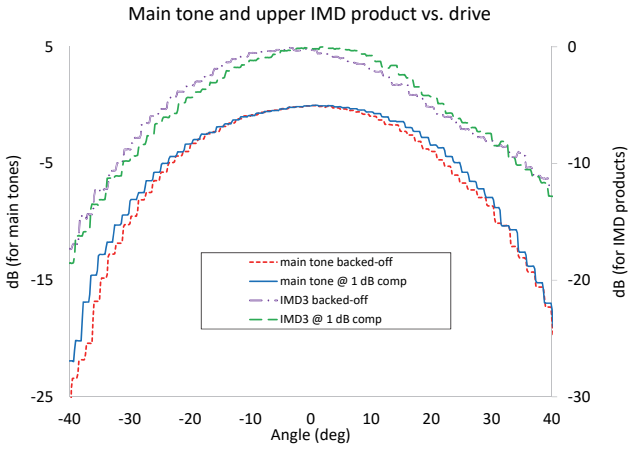

Figure 7 Main tone and intermodulation product patterns are shown here for two different levels of compression.

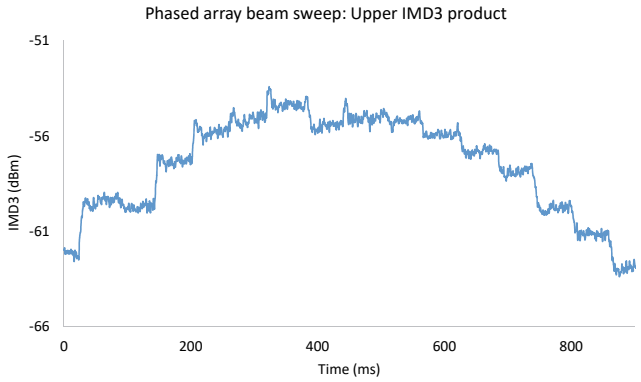

Figure 8 A detailed beam sweep pattern for an array is shown here (1 degree programming steps) but of a 3rd order intermodulation product. Note the overshoot dynamics in places and the overall asymmetry.

4 Conclusions

A less-visited aspect of phased array measurement relates to the dynamics of beam transitions both on the main transmitted signals and on distortion products. A sufficiently flexible measurement system (in terms of acquisition rates, triggering methods and receiver configuration) can enable the capture of this class of information. Such results can help quantify system performance more accurately in the fast steering limits.

References

1) J. S. Herd and D. Conway, "The evolution to modern phased array architectures," *Proc. IEEE.,* vol. 104, pp. 519-529, Mar. 2016.
2) P. Choi, D. A. Antoniadis and E. A. Fitzgerald, "Towards millimeter-wave phased array circuits and systems for small form factor and power efficient 5G mobile devices," *2019 IEEE Symp. On Phased Array Sys. And Tech.*, June 2019, pp. 1-4.
3) A.B. Smolders, A.C.F. Reniers, U. Johannsen, and M.H.A.J. Herben, "Measurement and calibration challenges of microwave and millimeter-wave phased-arrays," *2013 Int. Wkshp. On Ant. Tech.*, June 2013, pp. 1-4.
4) M. Jokinen, O. Kursu, N. Tervo, J. Saloranta, M. E. Leinonen, and A. Pärssinen, "Over-the-Air Phase Measurement and Calibration Method for 5G mmW Phased Array Radio Transceiver," *93rd ARFTG Conf. Dig.*, June 2019, pp. 1-4.
5) J. Henrie and M. Tang, "Measurement of time-evolving electronically steerable radiation patterns at fast timescales by a sampling technique," *2011 IEEE MTT-S Int. Micr., Symp. Dig.*, June 2011, pp. 1-4.
6) C. Fager, K. Hausmair, K. Buisman, K. Andersson, E. Sienkiewicz, and D. Gustafsson, "Analysis of nonlinear distortion in phased array transmitters," *2017 Integ. Nonlinear Micr. And mm-wave Circ. Wkshp. (INMMiC)*, Apr. 2017, pp. 1-4.
7) J. Martens, "Transient phased array distortion measurements," *to be presented at the 2021 Eur. Micr. Conf.*, Feb. 2022.
8) J. Martens and T. Roberts, "Broadband 220 GHz network analysis: structures and performance," *94th ARFTG Conf. Dig.*, Jan. 2020, pp. 1-4.
9) J. Martens, E. Vayner and J. Tu, "Towards Faster, Swept, Time-Coherent Transient Network Analyzer Measurements," *86th ARFTG Conf. Dig.*, Dec. 2015, pp. 1-4.
10) J. Martens, "On MM-wave quasi-linear over-the-air modulated measurements and coupling effects", *2017 47th European Microwave Conference (EuMC)*, Oct. 2017, pp. 1005-1008.

Author

Jon Martens
Service Infrastructure Solutions
US Division
Measurement Business Division

Publicly available